ISSN 0915-633X

NATIONAL INSTITUTE FOR FUSION SCIENCE

X-ray Spectra from Hinotori Satellite and Suprathermal Electrons

T. Kato and K. Masai

(Received – Sep. 21, 1992)

NIFS-197 Oct. 1992

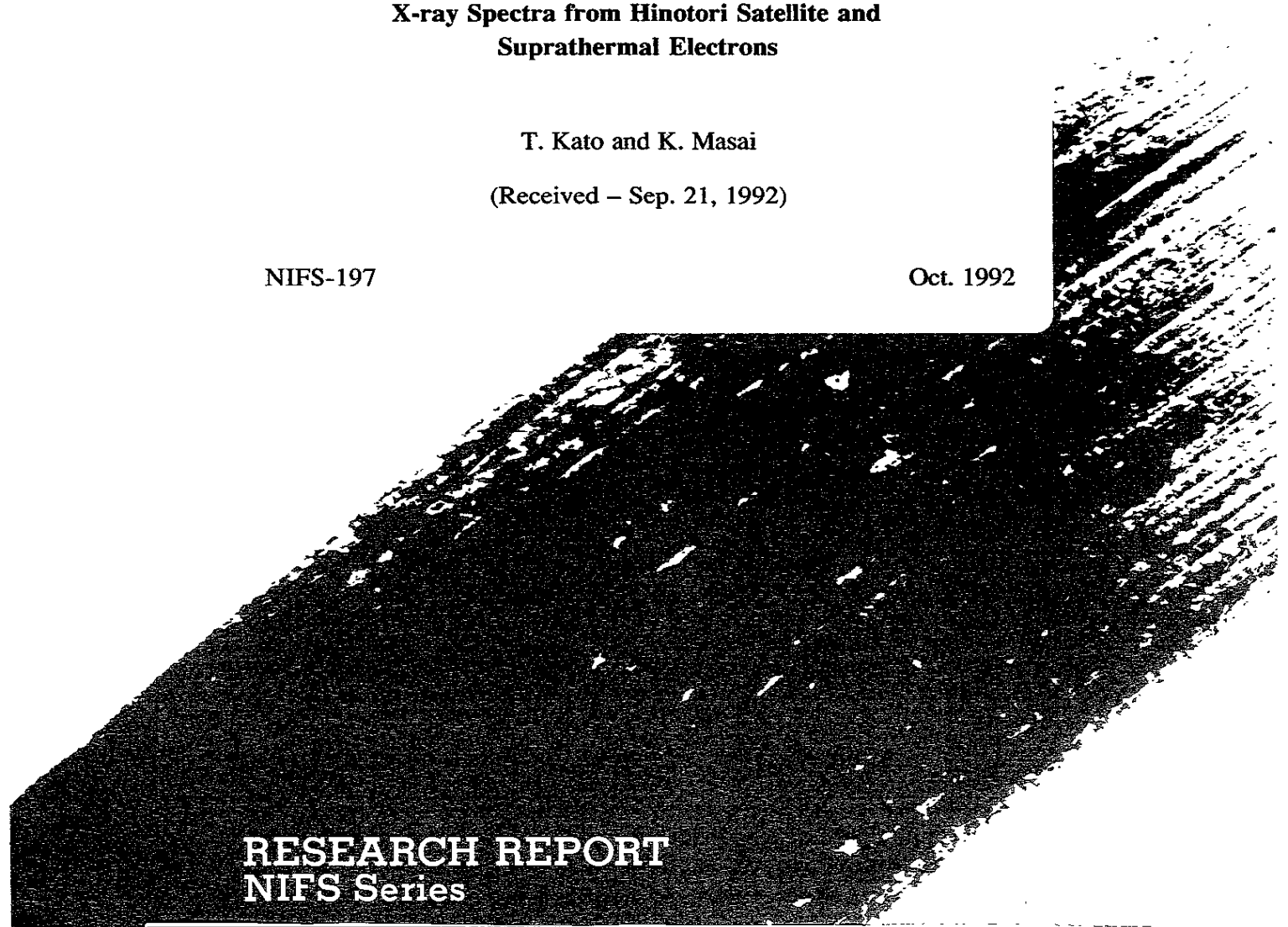

RESEARCH REPORT
NIFS Series

NAGOYA, JAPAN

X-ray Spectra from Hinotori Satellite and Suprathermal Electrons

Takako KATO and Kuniaki MASAI
National Institute for Fusion Science,
Nagoya 464-01

Abstract

We analyzed the X-ray spectra of H-like and He-like iron ions from a solar flare observed by Hinotori satellite, taking into account of a possible contribution of high energy electrons. The time behaviour of the relative densities of iron ions was calculated for a plasma of non- equilibrium ionization in the presence of suprathermal electrons of a few percent fraction. This model can reproduce the time evolution of the H-like and He-like spectra consistently.

Key words

solar flares, X-ray spectrum, He-like and H-like iron ions, suprathermal electrons

1. Introduction

The high resolution X-ray spectra of highly ionized H-like and He-like iron ions from solar flares were observed by the Hinotori satellite(Tanaka 1986). By the spectral analysis, the ion temperature and the electron temperature as well as the ion density ratios can be obtain from the satellite lines (Gabriel 1972). Several problems have been found in the theoretical fitting to the data by Hinotori satellite as follows (Tanaka 1986,1987).

1)The discrepancy of the ion density ratios.

The ion density ratio n(H)/n(He) obtained from the observed He-like spectra is always higher than that expected from the ionization equilibrium for the electron temperature obtained from the intensity ratios of the satellite lines to the resonance line of He-like spectra. Here n(H) and n(He) are the ion densities of H-like and He-like iron ions, respectively. The ion density ratio n(H)/n(He) obtained from the intensity ratio of the resonance line of H-like ions to that of He-like ions gives also the same results.

2)The inconsistency of the electron temperatures.

The time dependent electron temperatures were derived from the intensity ratios of the dielectronic satellite lines to the resonance line of the both H-like and He-like spectra. The derived electron temperature from H-like ions T_e(H) is often higher than T_e(He) derived from He-like spectra near the peak temperature. Generally, two values are nearly equal to each other in the early and the later phase of the flare. The difference of the temperature is about factor of 2 at maximum.

3)The observed intensity of the intercombination line y ($1s^2\ ^1S$ - 1s2p

$^3P_1$) is generally larger than the theoretical values by 30 - 40 %. The similar anomaly were also observed in the spectra from tokamak plasmas for He-like Ti ions. (Bitter 1985, Kato et al 1987, 1988) . It might be necessary to check the atomic data of the transition probabilities etc.

4)The intensities of the satellite lines of n = 3 sometimes show larger values than the theoretical values, especially at low temperature phases.

5)The intensity ratio of the Lyα_1 to that of Lyα_2 line of H-like ions is estimated to be 2 theoretically, but sometimes the ratio is smaller than 2 and dose not exceed 2.

In order to solve the problems (1) and (2), we propose a plasma model of time dependent ionization with suprathermal electrons in this paper .

2. Atomic data

The problems (1) and (2) in Sec.1 are related to the uncertainty in the atomic data for calculating the ion density ratios in ionization equilibrium as well as for deriving the electron temperature from the line intensity ratios of the satellite lines to that of the resonance line. Theoretical data for H- like (Fe^{25+}), He - like (Fe^{24+}) and Li - like (Fe^{23+}) ions are compared.

1)Ionization rate coefficients

Empirical formulae by Lotz(1967) are widely used. The differences between the calculation by Younger (1982) with DW (Distorted Wave) method are in agreement within 10% (Kato et al. 1991). We have to pay an attention that the coefficients in Table 2 of Younger(1982) are given in $\pi a_0^2 Ryd^2$ and not $10^{-14}\,cm^2\,eV^2$ as stated due to the misprint. Then the parameters in wrong unit give the smaller values by 60% than DW values.

2) Recombination rate coefficients

The differences between Jacobs (1977) and Arnaud & Rothenflug (1985) are within 40%.

3) Excitation rate coefficients

The differences among Bely- Dubau (1982), Safronova and Pradhan(1985) are within 7% for the resonance line w of He-like ions. The difference for the forbidden line z ($1s^2\ ^1S$ - $1s2s\ ^3S$) between Bely- Dubau (1982) and Pradhan(1985) is about 35% at low temperature near 1 keV (Kato 1989). For the Lyα line of H-like ions, the difference between Bely-Dubau (1982) and Callaway (1985) is 10% near 1 keV.

4) Satellite lines

For iron ions, the data by Bely- Dubau (1982) and Dubau (1981) are compared with recent results by Safronova (1992). The differences between Bely- Dubau (1982) and Safronova (1992) are 8% and 40% for the line j ($1s^2 2p\ ^2P_{2/3}$ - $1s2p^2\ ^2D_{5/2}$) and n = 3 ($1s^2 3l$ - $1s2l'3l'$) dielectronic satellite lines, respectively. This difference is not effective for the present analysis since the electron temperature is derived from I_j / I_w, but is important for the temperature diagnostics using the intensity ratios of the n=3 satellite lines to the resonance line. The satellite intensities by Safronova (1992) are always larger than those by Bely- Dubau (1982). As a result, the data by Safronova gives a higher electron temperature than by Bely-Dubau by 0.1 keV at 1.5 keV. For H-like ions, the values in Safronova (1992) are also larger than those in Dubau (1981) by 40% for n=3 and 4 satellite lines. Since these satellite lines are too close to the Lyα line to resolve each other, the apparent intensity of $Ly\alpha_1$ is influenced by the satellite lines and differs differs 17% at 1.5 keV in the two calculations. This

results in a difference in the temperature deduced: the data by Dubau (1981) gives a temperature 0.1 keV higher than Safronova (1992). At temperatures higher than 2.5 keV, the difference is negligibly small. For the intensities of the satellite lines of He-like ions at 1.787 - 1.789 A ($1s2s\,^1S$ - $2s2p\,^1P_1$, $1s2p\,^3P$ - $2p^2\,^1D$, ^3P), the difference of 25% is found. The intensities of the strongest satellite lines near 1.792 A ($1s2p\,^1P_1$ - $2p^2\,^1D_2$, $1s2p\,^3P_2$ - $2p^2\,^3P_2$) agree within 6%.

Thus, the uncertainty in the atomic data is estimated to be about 40% at most. The discrepancies mentioned in Sec.1 can not be ascribed only to the uncertainty in atomic data. We use the data by Arnaud and Rothenflug (1985) for ionization and recombination rate coefficients , Bely- Dubau (1982) for the Li-like satellite line intensities and Safronova(1992) for He-like satellite line intensities in our analysis.

3. Observed spectra of the flare on October 7, 1981

We have analyzed the spectra and modeled the large flare on October 7, 1981. Time profiles of various quantities during this flare are shown in Fig.1 (Tanaka 1986). From the top, intensities of w (Fe XXV) line and Lyα (Fe XXVI) lines, the hard X-ray flux in 30-40 keV and 67 - 152 keV energy bands, the ion temperature T_i deduced from the Doppler broadening and the electron temperature T_e(H)(dashed line) and T_e(He) (solid line) , the emission measure (EM) and the ion abundance ratio n(H)/n(He).

In Fig.2, the ion ratio n(H)/n(He) derived from the spectral fit to a single component thermal plasma is plotted (closed circles) as a function of

the electron temperature varying with time. The electron temperatures are those derived from He-like spectra I_j / I_w every 70-second interval. The attached number indicates the order of the time evolution. The values expected for ionization equilibria are shown by the broken line, which is a monotonously increasing function of electron temperature. The derived ion ratios n(H)/n(He) show the complicated trajectory far from the equilibrium values from the rising phase through the decay phase of the electron temperature. The ion ratio n(H)/n(He) increases in the rising phase and decreases in the decay phase; the plasma exhibit an ionizing tendency in the rising phase (from the sequence No.1 to No.6) and a recombining one in the decay phase (from No.6 to No.14), yet the values are always higher than the equilibrium values, i.e. in recombining phase through the flare.

Now we see the H-like spectra. The electron temperatures $T_e(H)$ derived from the intensity ratios of the satellite lines to $Ly\alpha_1$, I_s / I_L are higher than those $T_e(He)$ from He-like spectra as shown in Fig.1. For example, at the period when the electron temperature is the highest, $T_e(He)$ = 2.1 keV, whereas $T_e(H)$ = 3.2 keV. In Fig.3, the correlation diagram of the intensity ratio I_j / I_w and H-like one I_s / I_L is shown by closed circles in the time sequence. The simple solid line indicates the values in the ionization equilibrium. The data points deviate from the value in the ionization equilibrium. From the beginning of the flare No.1 towards the temperature maximum No.6, the plasma seems to be going away from an ionization equilibrium. Fig. 3 shows that the intensity of Lyα line is stronger than that expected from an ionization equilibrium. We consider a possibility that this difference is due to the contribution of the recombination from bared nuclei for the H-like spectra. We derived the ion density ratio n(Z)/n(H) assuming

the same electron temperature as T_e(He) for H-like spectra, where n(Z) indicates the density of fully stripped ions. The effective recombination rate coefficient to produce the resonance line of H-like ions α^{eff}_L is much larger than that of He -like ions α^{eff}_w, although the excitation rate coefficient for w, C_w, is larger than that of Lyα, C_L, as shown in Fig.4. The contributions of cascade from highly excited states to C^{eff} and the recombination into the upper state of ions for α^{eff} are taken into account for both He-like ions (Fujimoto and Kato 1984) and H-like ions(Ljepojevic et al 1984). The comparison for the rate coefficients of C^{eff} and α^{eff} are shown in Fig.4. C_j and C_s in Fig. 4 represent the rate coefficients of the satellite line, j of Li-like ions and s of He- like ions, respectively. At temperatures below 3 keV, α^{eff}_L is larger than C_L. Thus the Lyα line can be produced much effectively through the recombination process in solar flare plasmas. The derived value of n(Z)/n(H) varies largely from 0 to 0.2. This can be compared to the value of n(H)/n(He) which varies only between 0.02 and 0.03. The open circles in Fig.2 represent the derived n(Z)/n(H) which are larger than the values in the ionization equilibrium by nearly two orders of magnitude.

4. Time dependent hot spot model

In order to account for the problems raised above, we consider a presence of higher energy electrons. We assume the suprathermal electrons closely interacting with thermal one which is nearly in an ionization equilibrium. This model does not mean such a superposition of thermal

plasmas of different temperatures as suggested by differential emission measure modelling. Interactions of suprathermal electrons with the thermal plasma and of thermal electrons with the suprathermal plasma are essential in modelling here. The ionization takes place very rapidly in a suprathermal plasma.

$$d\,n^S(i)/dt = S^S(i-1)n^S(i-1)n_e + \alpha^S(i+1)n(i+1)n_e - (S^S(i) + \alpha^S(i))n(i)n_e \qquad (1)$$

where S^S and α^S indicate the ionization and recombination rate coefficients from an i times ionized ion, $n^S(i)$ the density of an ion i, in the suprathermal plasma, respectively. We consider that the ion densities n^S are mixed into the thermal plasma. Then the highly ionized ions n(H) and n(Z) can exist in the plasma of lower temperature and these ions can emit recombination lines effectively. The ion densities are written with a fraction of the suprathermal electrons η as,

$$\begin{aligned} n(He) &= n^0(He)(1-\eta) + n^S(He)\eta \\ n(H) &= n^0(H)(1-\eta) + n^S(H)\eta \qquad (2) \\ n(Z) &= n^0(Z)(1-\eta) + n^S(Z)\eta \end{aligned}$$

where n^0 indicates the densities in the thermal plasma. We assume that $n^0(i)$ is in the ionization equilibrium in thermal plasma of the temperature $T_e(He)$. Roughly speaking $n(H) \sim n^S(H)\eta$ and $n(He) \sim n^0(He)$, then η is estimated to be of the order of n(H)/n(He), taking $n^S(H) \sim 1$ and $n^0(He) \sim 1$.

We calculate the time dependent ion abundances (Masai 1984) with an 8 keV suprathermal component assuming a Maxwellian distribution of $\eta = 0.03$. Then H- like and fully stripped ions can be produced rapidly at the beginning of the flare. We assume that the suprathermal electrons of 8 keV exist constantly form No.1. to No.9 with $\eta = 0.03$, decrease to $\eta = 0.01$ at No.10 and disappeared in the later phase of the flare at No.12. The ion density ratios n(Z)/n(He), n(H)/n(He) and n(Li)/n(He) obtained from this calculation are plotted as a function of T_e in Fig.5. The solid lines represent the calculated result and the dotted lines represent the values in ionization equilibria. The arrows indicate the direction of time. The presence of 8 keV suprathermal electrons of 3% enhances the ion ratios to be much larger than in the ionization equilibrium.

In the suprathermal plasma, iron is ionized to be He-like or more and the ion abundances of the low ionized ions with L-shell electron such as Li - like ions are negligible. Then the abundances of these low ionized ions by eq.(2) are not affected by the presence of suprathermal electrons and close to the ionization equilibrium values, as shown in Fig. 5. .

The resonance line intensity for He-like ions can be expressed as,

$$I_w = (C_{w0}^{eff}(1-\eta) + C_{ws}^{eff}\eta)n(He)n_e + \alpha_w^{eff}(1-\eta)n(H)n_e \quad (3)$$

where C_{w0}^{eff} and C_{ws}^{eff} mean the effective excitation rate coefficients at the temperature T_e in the thermal plasma and T_s in the suprathermal plasma, respectively. α_w^{eff} indicates the effective recombination rate coefficient to produce the resonance line. This rate is large at low temperatures and is negligible in the suprathermal plasma. On the intensity

of the satellite lines like I_j, the effect of the suprathermal electrons is small and no contribution from recombination.

The ion density ratios derived from the spectra taking into account the contribution of the suprathermal electrons and the recombination according to eq.(3) are also plotted in Fig.5 by open and closed circles for n(Z)/n(He) and n(H)/n(He), respectively, and triangles for n(Li)/n(He). The electron temperature takes the values T_e = 1.65 - 1.8 keV which are lower than those derived without suprathermal electrons.

In order to be consistent with the observed spectra which can be fitted well by thermal electrons, the effect of the high energy electrons on the spectra should be examined. The forbidden line intensity I_z has three origins; the excitation of He-like ions, the inner-shell ionization of Li-like ions and the recombination of H-like ions.

$$I_z = (C_{z0}^{\mathrm{eff}}(1-\eta) + C_{zs}^{\mathrm{eff}}\eta)\, n_e n(\mathrm{He}) + (S_z^0(1-\eta) + S_z^s\eta)\, n_e n(\mathrm{Li}) + \alpha_z^{\mathrm{eff}}\, n_e n(\mathrm{H}) \qquad (4)$$

where S_z^0 and S_z^s indicate the ionization rate coefficients to produce the forbidden line z through the inner-shell ionization. The line q is produced predominantly by the inner-shell excitation of Li-like ions whereas the line j and k arises from dielectronic recombination of He-like ions only. The contributions of the excitation and inner-shell ionization by suprathermal electrons and the recombination in the thermal plasmas for the spectra are shown in Figs. 6 and 7 by dot-dashed lines and dashed lines (with shaded), respectively. Fig.6 and 7 show the spectrum for He-like ions and H-like ions

for three phases; (a) early phase (No.3), (b) middle phase(No.6) and (c) late phase (No.13), respectively.

The energy distribution of suprathermal electrons is assumed to be Maxwellian distribution in our calculation. The electron energy should be larger than the ionization potential of H-like ions, 9.3 keV, in order to produce the bare nucleus, and would be necessary greater than 10 keV to produce highly charged ions effectively when the suprathermal electrons have a sharp energy distribution. However the energy of 10 keV is not good for the spectral fit of He-like ions because the influence is too high for the line intensities for which excitation energies are around 6.7 keV. The energies where the cross section has the maximum value for the excitation and ionization are about 10 keV and 20 keV respectively. Since the low energy is better to fit the observed spectra, the broad band distribution in energy for the suprathermal electrons is more probable to explain both the spectra and ion abundances.

4. Discussions

Introducing a small amount of suprathermal electrons we calculate time dependent ionization to explain the time variation of the spectra of both He-like and H-like ions . We can explain the time behaviour of the spectra, the ion density ratios and the electron temperature simultaneously. We discuss the problems remaining in our model.

1)Ionization time

Generally it takes $n_e t^* \sim 10^{12}$ cm^{-3} s to reach the ionization equilibrium (Masai 1984). The density in the solar flare is estimated to be around 10^{11} cm^{-3} (Tanaka 1986). When there is no flow from outside, plasma would be in the ionization equilibrium in ~10 s which is much

shorter than the duration time ~10 min. of the solar flare. If the plasma is not in the ionization equilibrium as mentioned in the previous section, the following possibilities can be considered.

(a) the density of the plasma is less than 10^{10} cm^{-3}, or

(b) there are relative dynamic motions in the plasma.

Since the time when the temperature reaches the maximum $t_p \sim 400s$, n_e is smaller than 3×10^9 cm^{-3} in the case of (a). In the case of (b), the characteristic velocity of dynamics is written $v \sim (L_T / t_p^*)(1 - t_p^*/t_p)$ where the scale length of the temperature $L_T \sim (\nabla \ln T_e)^{-1}$. Since $t_p^* \sim 10^2 (n_e/10^{10})^{-1}$, $v \sim 200$ - 300 km/s for $n_e = 10^{10} cm^{-3}$, $L_T \sim L_x/2 \sim 3 \times 10^9$ cm where L_x is the width measured by X -ray telescope. This value is may be consistent with to the measured value ~ 400 km/s from the wavelength shift of the resonance line of the He-like ions at the beginning of a flare (Tanaka 1987).

2) Suprathermal component and continuum X rays

The volume ratio of the suprathermal electrons to the thermal electrons is about 3%. The ratio in energy is 20 - 30 %. Generally continuum X ray spectrum shows thermal type at low energies (< 5 keV) whereas power type at high energies. The continuum X ray spectrum 30 - 300 keV measured on the October 7 1981 shows large excess around 30 - 40 keV, when the power spectrum is extrapolated to the lower energy regions from higher energy regions. This excess part may related to the suprathermal electrons, introduced in our model.

3) We have made a model that the X-ray spectra of H-like ions and He-like ions are produced in a same plasma although the apparent electron

temperature, Te(H) and Te(He), derived from the spectra is different The line intensity ratio I_w / I_L obtained from the model is in agreement with the measurements within a factor of 5 The discrepancy is large at the beginning of the flare and decrease towards the later phase.

References

M. Arnaud and R. Rothenflug, Astron. Astrophys. Suppl. 60 (1985) 425}

F. Bely-Dubau, J. Dubau, P. Faucher and A.H. Gabriel, Mon. Not. Roy. Astron. Soc.,198 (1982) 239}

M. Bitter, K.W. Hill, M. Zarnstorff, S. von Goeler, R. Hulse, L.C. Johnson, N.R. Sauthoff, M. Tavernier, F. Bely-Dubau, P.Faucher, M. Cornille and J. Dubau, Phys. Rev. 32 (1985) 3011

J. Callaway, Physics Letters 96A (1985) 83}

J. Dubau, A. H. Gabriel, M. Loulerque, L.Steenman- Clark and S. K. Volonte, Mon. Not. Roy. Astron. Soc.,195 (1981) 705}

T. Fujimoto and T. Kato, Phys. Rev. A 30 (1984) 379}

A.H. Gabriel, Mon. Not. Roy. Astron. Soc. 160 (1972) 885

V.L. Jacobs, J. Davis, P.C. Kepple and M. Blaha, Astrophys. J. 211 (1977) 605}

N.N. Ljepojevic, R.J. Hutcheon and R.W.P. McWhirter, J. Phys. B 17 (1984) 3057}

W. Lotz, IPP 1/62 (1967)

K. Masai, Astrophys. Space Sci. 98 (1984) 367

T. Kato and S. Nakazaki, Atomic Data & Nuclear Tables, 42,313(1989)

T. Kato, K. Masai, Journal de Physique C1, Suppl. No.3 49 (1988) C-349}

T. Kato, K. Masai and M. Arnaud, NIFS-DATA-14 (1991)

A.K. Pradhan, Ap. J. Suppl. 59 (1985) 183}

U. Safronova, Private communication (1992)}

K. Tanaka, Publ. Astron. Soc. Japan 38 (1986) 225}

K. Tanaka, Publ. Astron. Soc. Japan 39 (1987) 1}

S. M. Younger, Quant. Spectrosc. Radiat. Transfer 26 (1981) 329}

Figure Captions

Fig.1..Various time profiles for the flare of 7 October 1981. From the top, relative intensity time profiles of w line and Lya lines of Fe ions, and the hard X-ray flux profiles of 30-40 keV and 67 - 152 keV, ion temperature T_i and electron temperature T_e(H)(dashed line) and T_e(He) (solid line) , emission measure (EM) and ion abundance ratio n(H)/n(He) (Tanaka 1986).

Fig.2 The ion density ratios against the electron temperature. Ion density ratios n(H)/n(He) and n(Z)/n(He) of Fe ions derived from the spectra assuming only with thermal plasma are plotted by closed and open circles, respectively for the solar flare spectra on 7 October 1981 . Dashed lines are the values in the ionization equilibrium.

Fig.3. The correlation diagram of the intensity ratios of I_s/I_L and I_j/I_w. The closed circles are obtains from the spectra following the time sequence. The solid line indicates the value in the ionization equilibrium..

Fig. 4 The effective excitation and recombination rate coefficients to produce the line emission of Lya(H-like) and w (He-like). The rate coefficients for the satellite lines of H-like(s) and He-like(j) ions are also shown,

Fig.5 The ion density ratios for Fe ions against the electron temperature taking into account the suprathermal electrons. The solid lines indicate the calculated results. The arrows indicate the direction of the time. The close and open circles are obtained from the spectra including the contribution of the suprathermal electrons.

Fig.6 The observed spectra(histo gram) and calculated ones(solid line) for He-like ions for three phases; (a).the early phase (22H56m39S - 22H57m49s), (b) the middle phase (23H0m8s - 23H1m18s), (c) the late phase (23H 8m41s - 23H 9m51s). Dashed lines show the contribution of the recombination and dot- dashed lines of the excitation, inner-shell excitation and inner-shell ionization by the suprathermal electrons.

Fig.7. Same as Fig.6 but for the spectra of H-like ions.

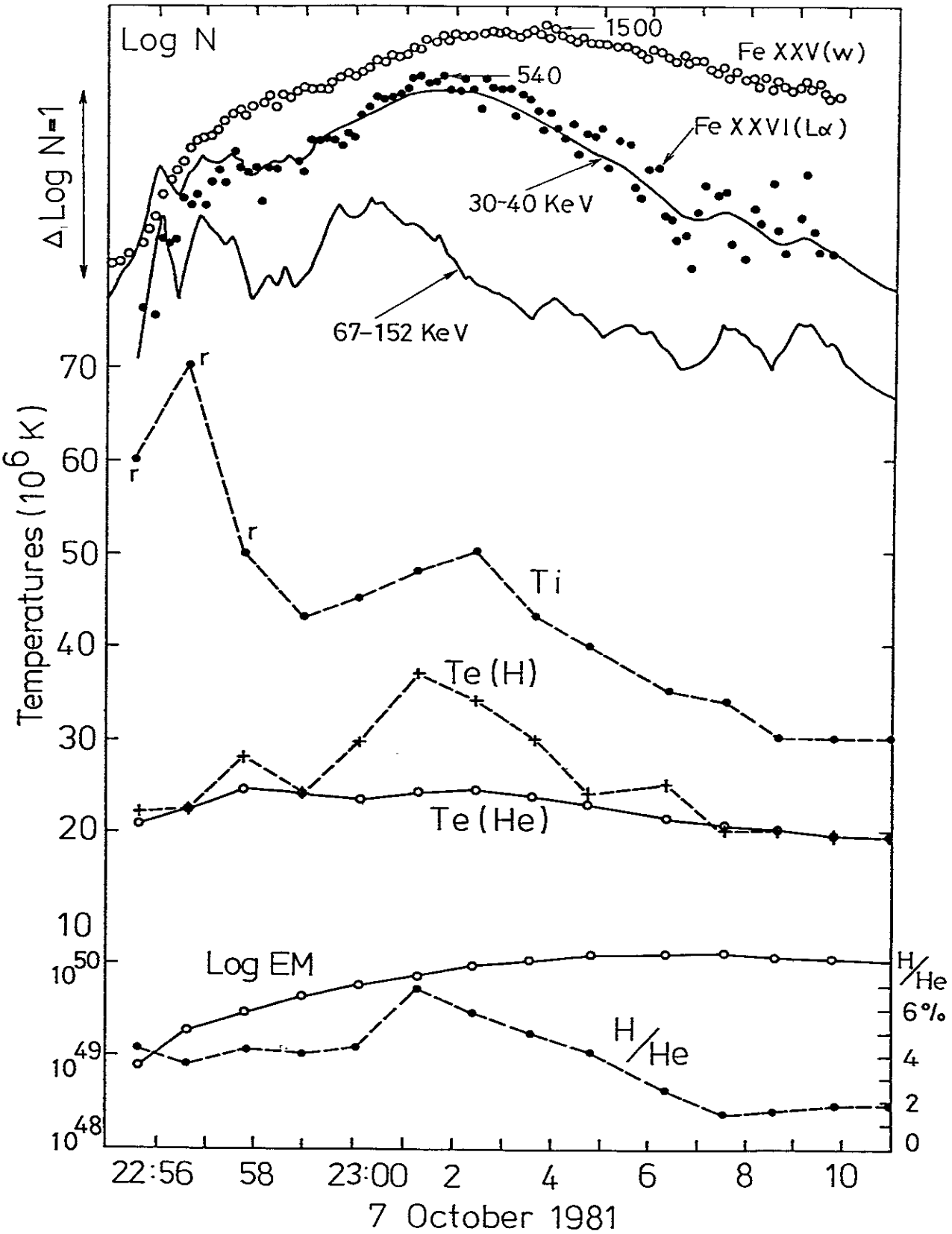
Log N
1500
Fe XXV(w)
540
Fe XXVI(Lα)
30-40 KeV
67-152 KeV
Δ Log N=1
Temperatures (10^6 K)
70
60
50
40
30
20
10
r
r
r
Ti
Te (H)
Te (He)
Log EM
10^{50}
10^{49}
10^{48}
H/He
6%
4
2
0
22:56
58
23:00
2
4
6
8
10
7 October 1981

Fig.1

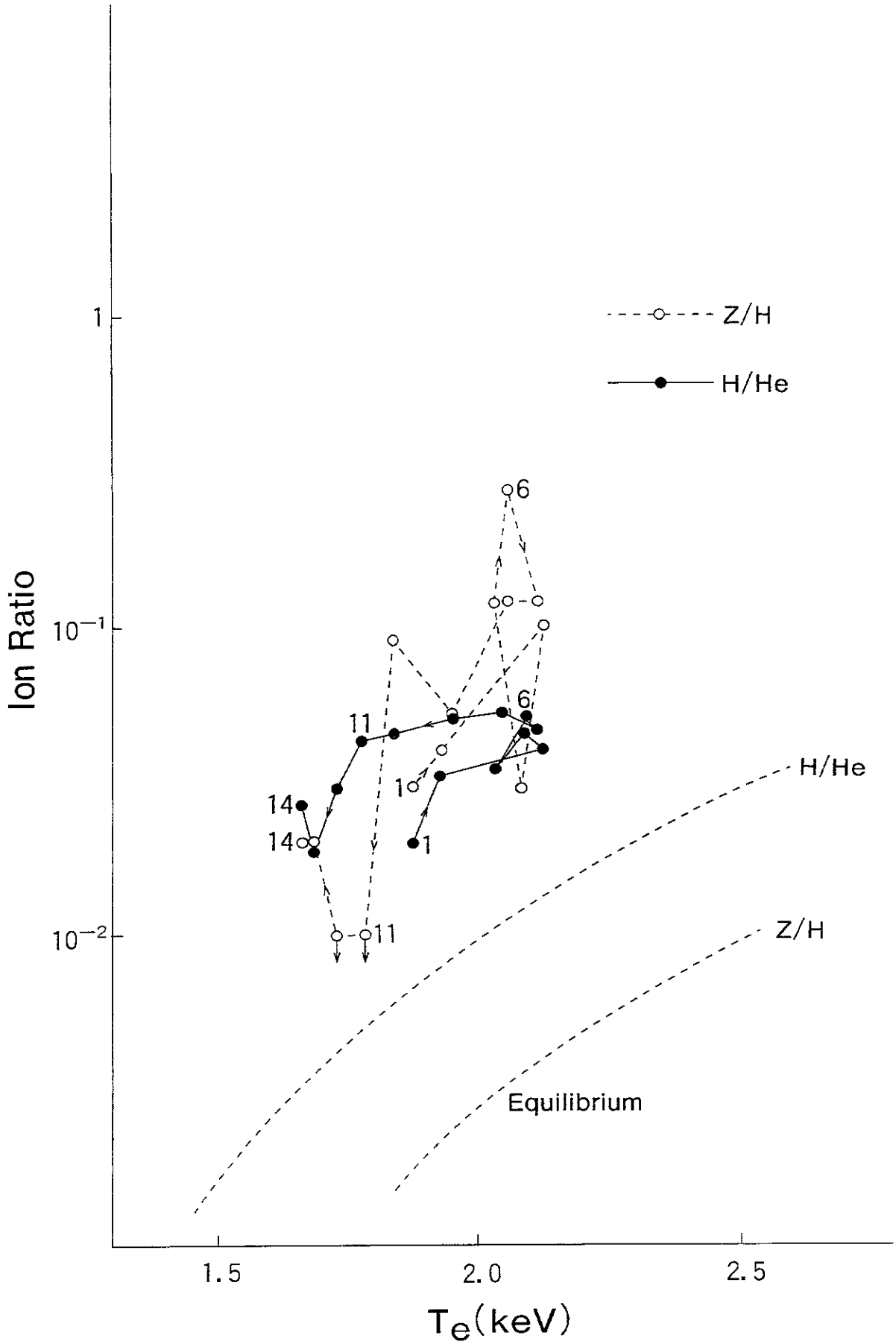
Z/H
H/He
Ion Ratio
1
10^{-1}
10^{-2}
6
11
14
14
1
6
11
1
H/He
Z/H
Equilibrium
1.5
2.0
2.5
T_e(keV)

Fig.2

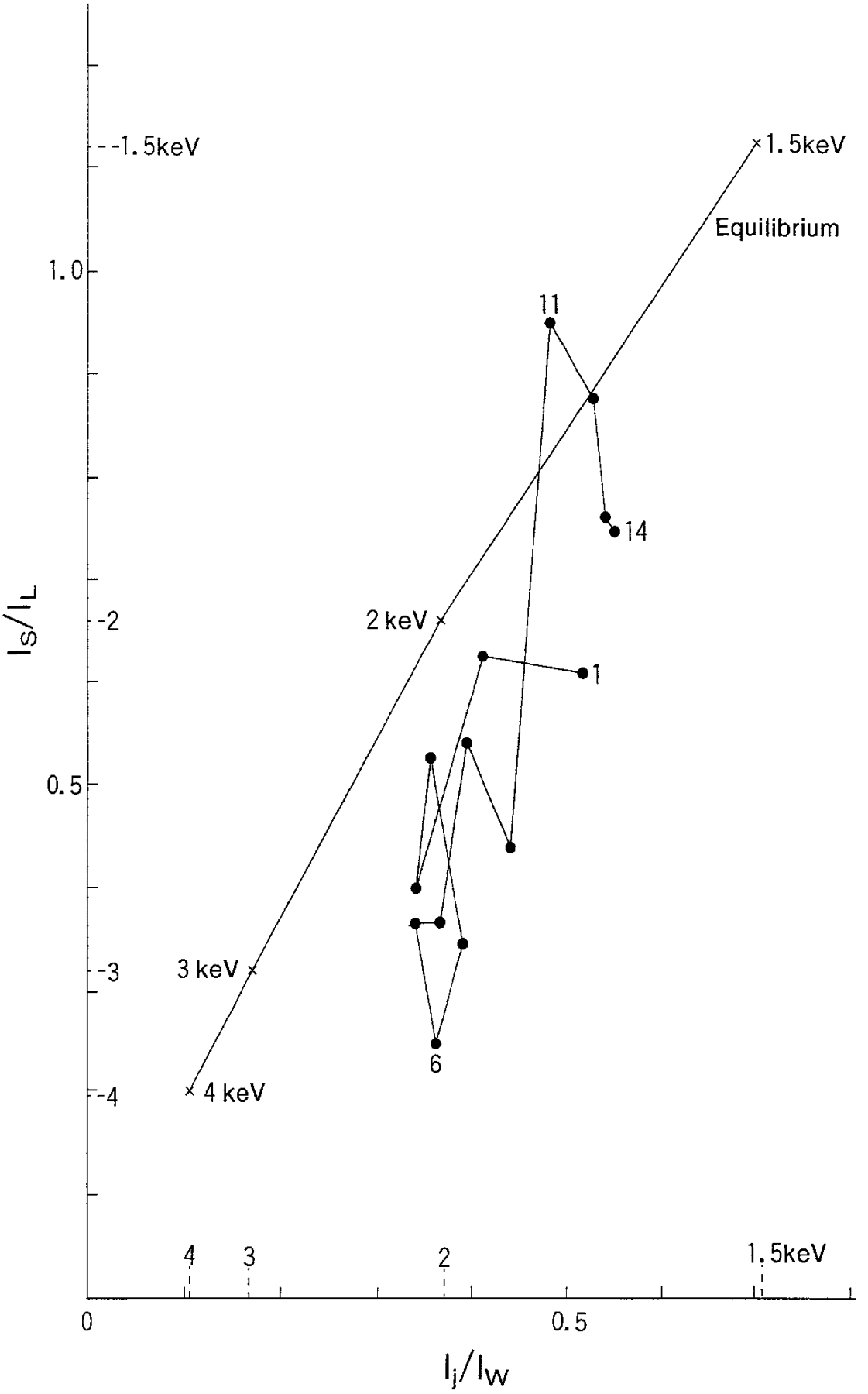
1.5keV
Equilibrium
1.5keV
1.0
11
14
2 keV
1
0.5
3 keV
6
4 keV
4
3
2
1.5keV
0
0.5
I_S/I_L
I_j/I_W

Fig.3

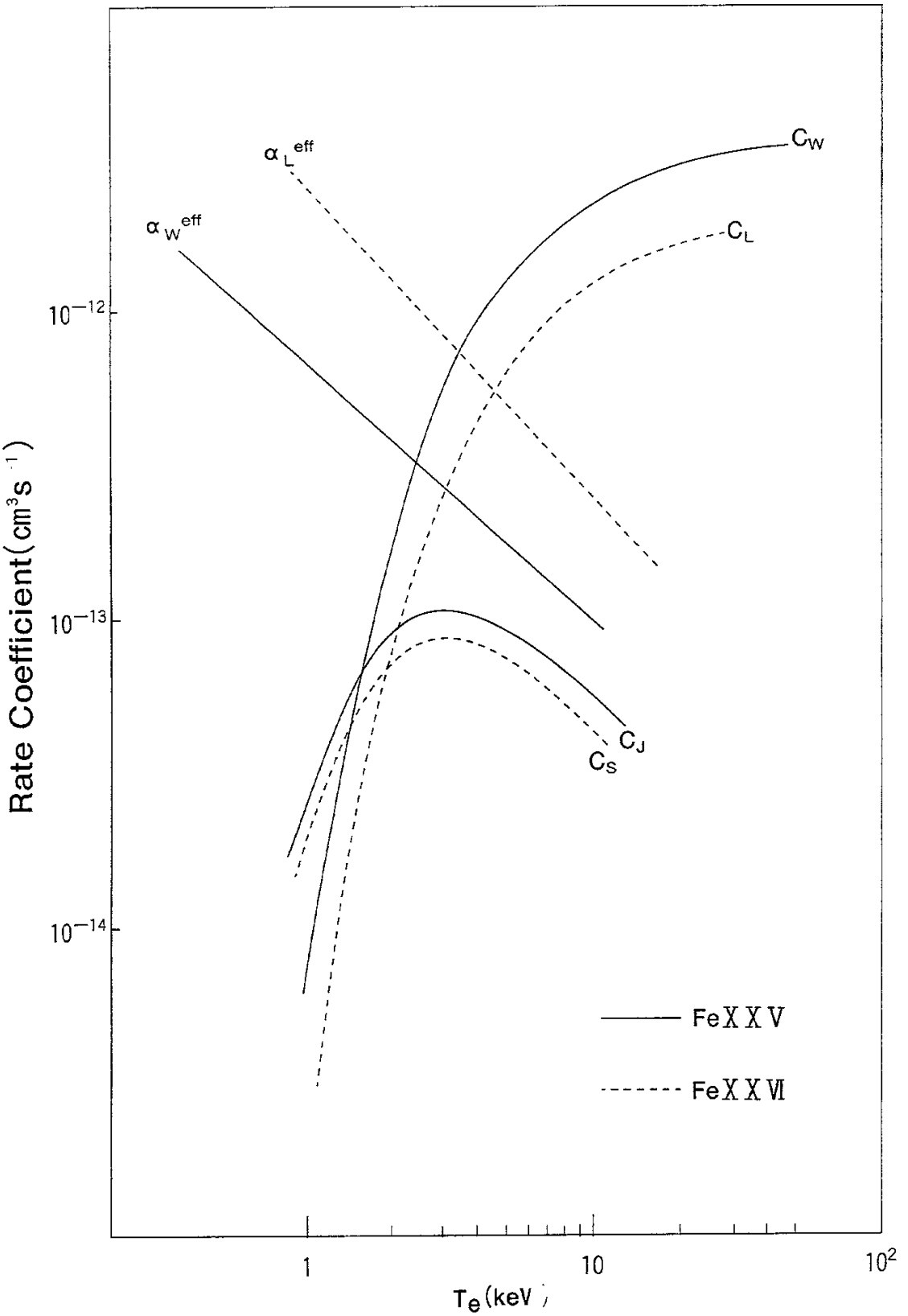
Rate Coefficient(cm³s⁻¹)
10⁻¹²
10⁻¹³
10⁻¹⁴
α L eff
α W eff
C W
C L
C J
C S
FeXXV
FeXXVI
1
10
10²
Te(keV)

Fig.4

Fig.5

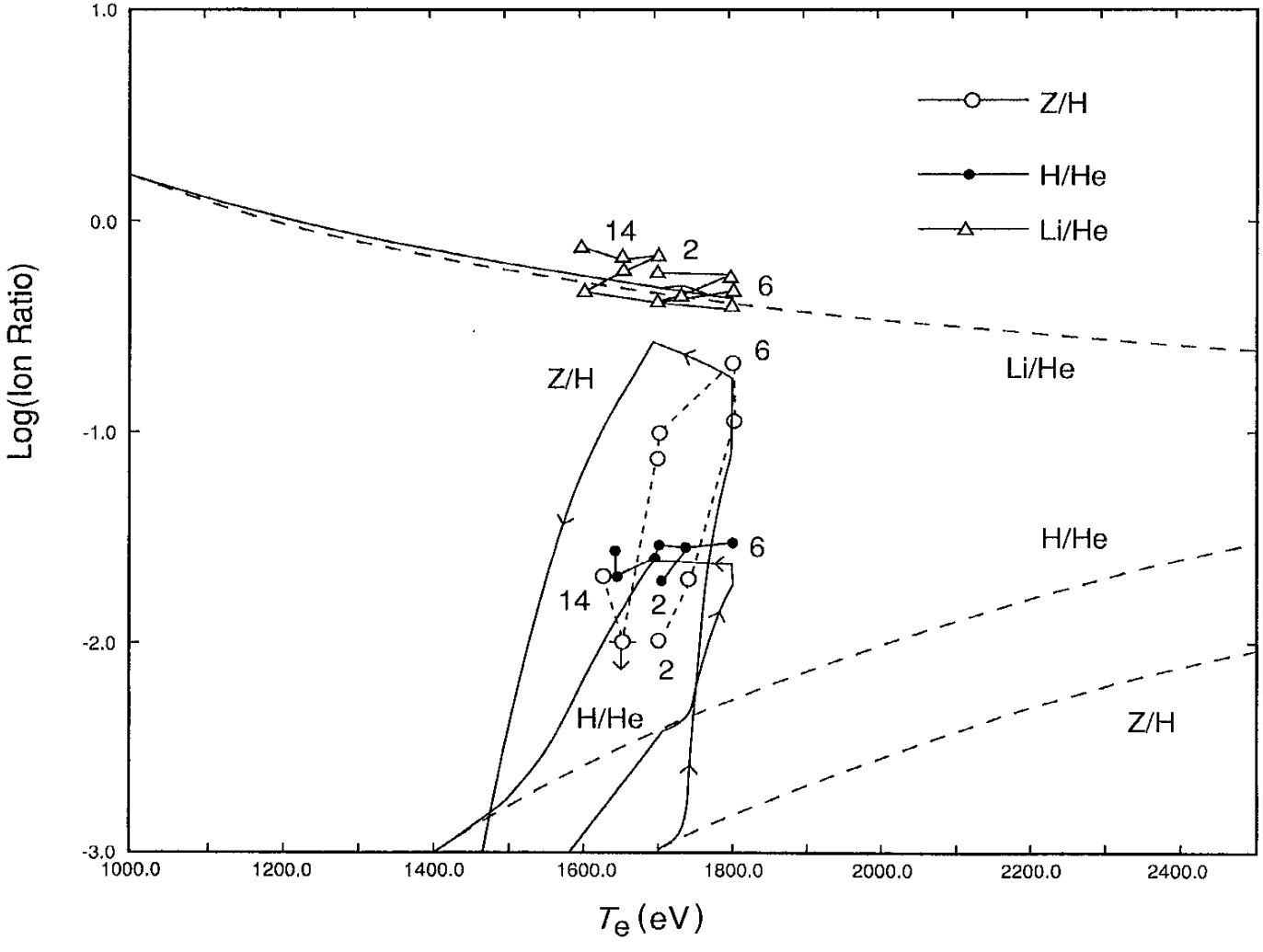
1.0
0.0
-1.0
-2.0
-3.0
Log(Ion Ratio)
1000.0
1200.0
1400.0
1600.0
1800.0
2000.0
2200.0
2400.0
T_e (eV)
Z/H
H/He
Li/He
14
2
6
Z/H
Li/He
H/He
Z/H
H/He

Fig.6 (a)

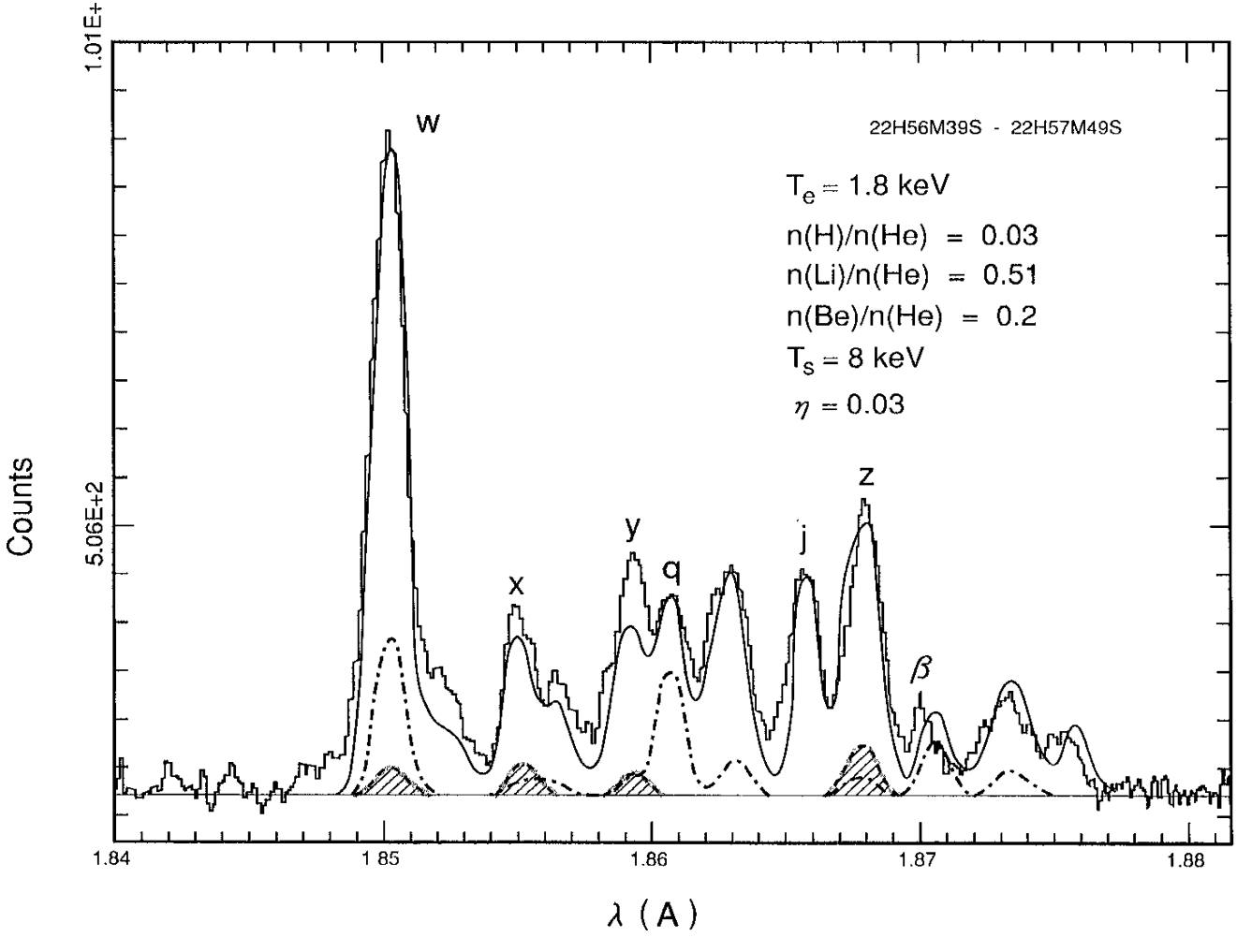
1.01E+
5.06E+2
Counts
22H56M39S - 22H57M49S
T_e = 1.8 keV
n(H)/n(He) = 0.03
n(Li)/n(He) = 0.51
n(Be)/n(He) = 0.2
T_s = 8 keV
η = 0.03
w
x
y
q
j
z
β
1.84
1.85
1.86
1.87
1.88
λ (A)

Fig.6 (b)

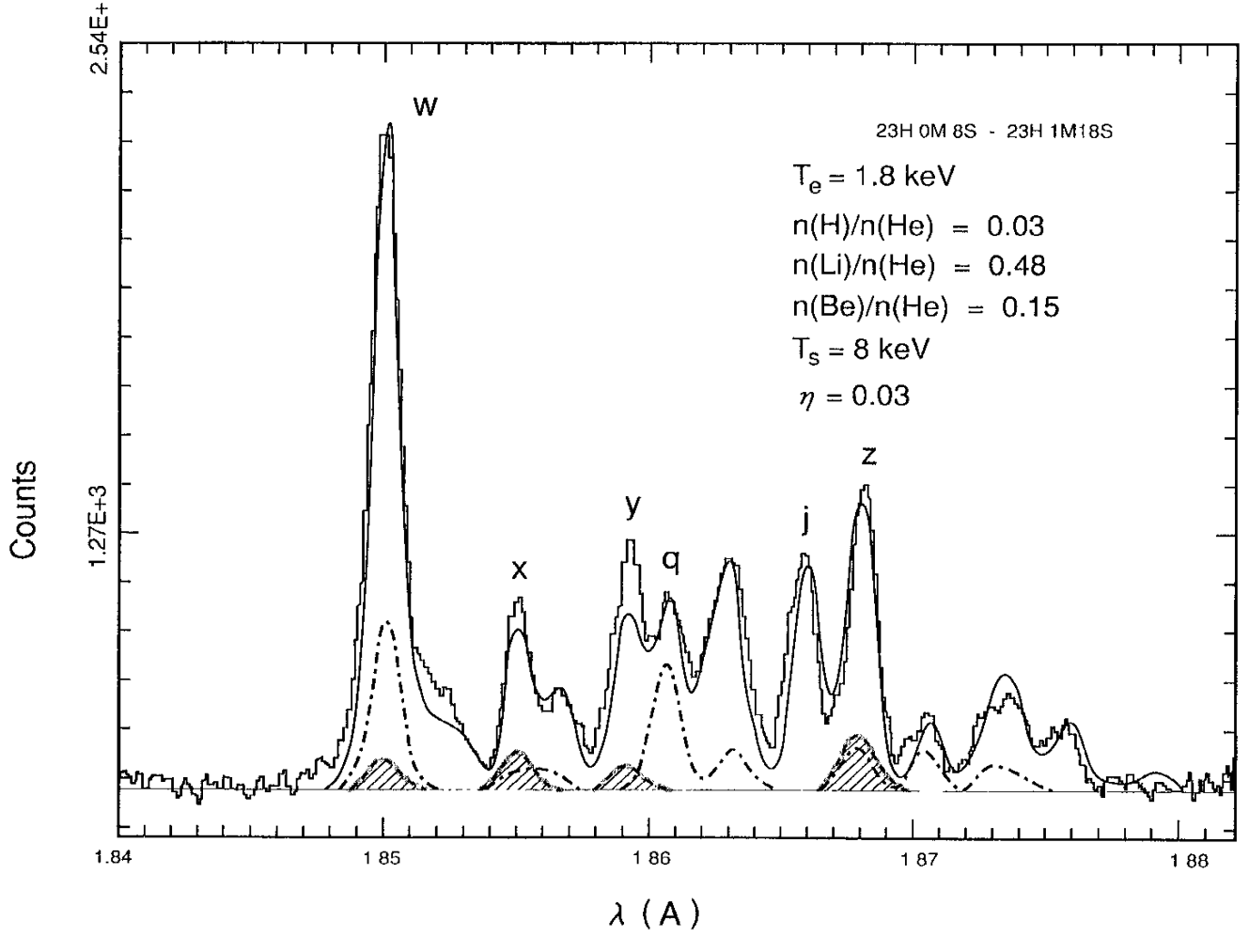
2.54E+
1.27E+3
Counts
w
x
y
q
j
z
23H 0M 8S - 23H 1M18S
T_e = 1.8 keV
n(H)/n(He) = 0.03
n(Li)/n(He) = 0.48
n(Be)/n(He) = 0.15
T_s = 8 keV
η = 0.03
1.84
1 85
1 86
1 87
1 88
λ (A)

Fig.6 (c)

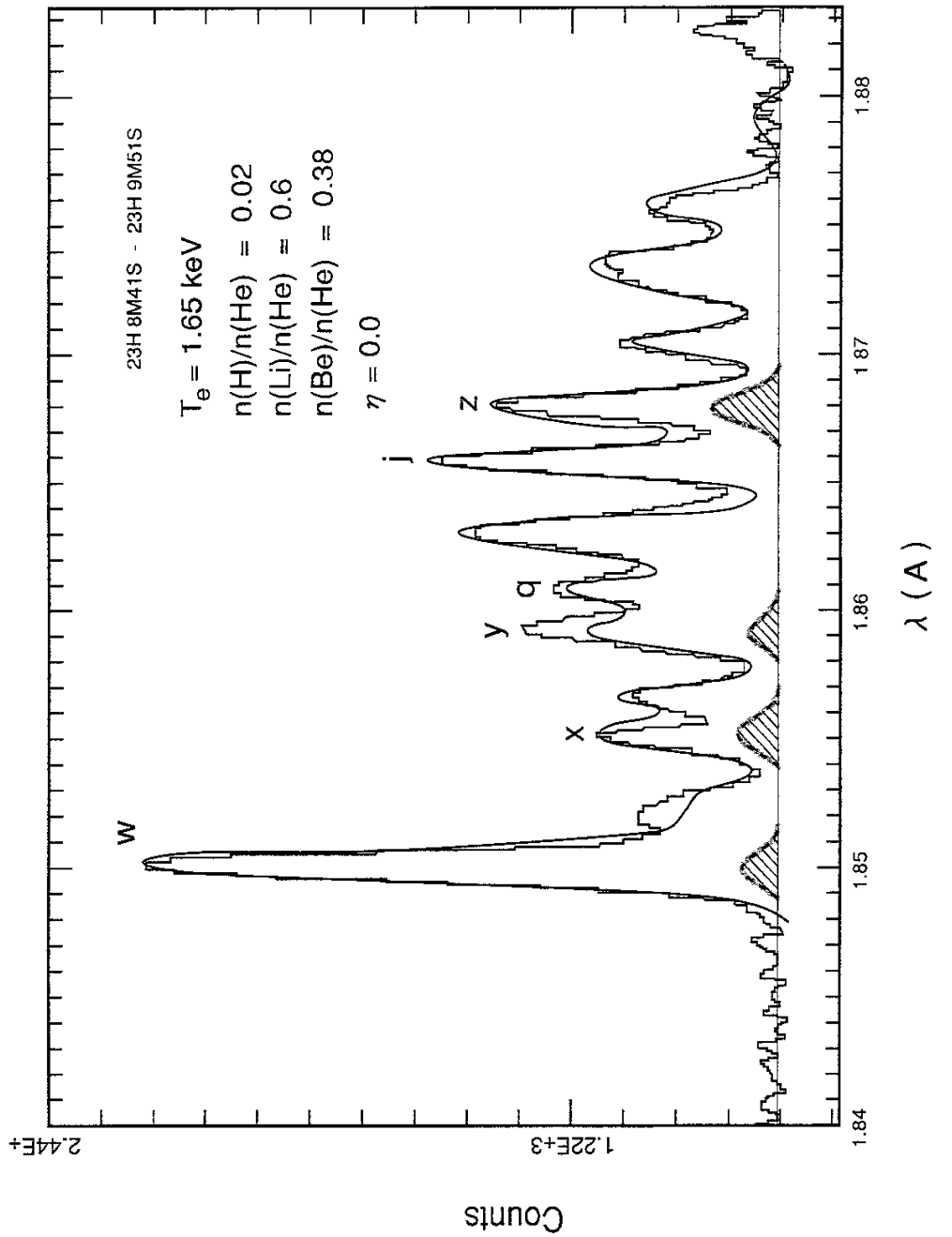
23H 8M41S - 23H 9M51S
T_e = 1.65 keV
n(H)/n(He) = 0.02
n(Li)/n(He) = 0.6
n(Be)/n(He) = 0.38
η = 0.0
w
x
y
q
j
z
Counts
2.44E+
1.22E+3
1.84
1.85
1.86
1.87
1.88
λ (A)

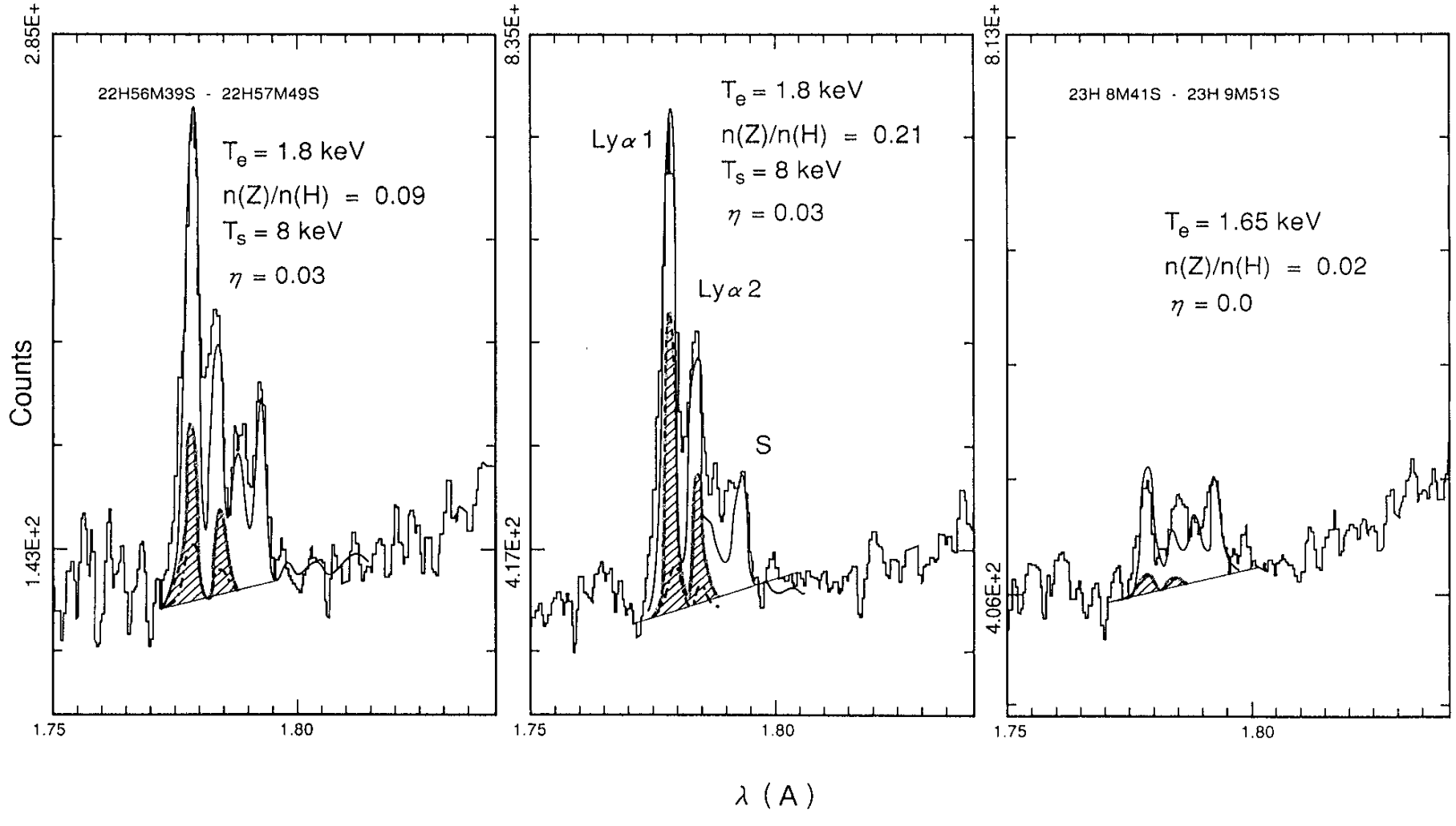
2.85E+
1.43E+2
Counts
22H56M39S - 22H57M49S
T_e = 1.8 keV
n(Z)/n(H) = 0.09
T_s = 8 keV
η = 0.03
1.75
1.80
8.35E+
4.17E+2
T_e = 1.8 keV
n(Z)/n(H) = 0.21
T_s = 8 keV
η = 0.03
Lyα 1
Lyα 2
S
1.75
1.80
8.13E+
4.06E+2
23H 8M41S - 23H 9M51S
T_e = 1.65 keV
n(Z)/n(H) = 0.02
η = 0.0
1.75
1.80
λ (A)

Fig.7

Recent Issues of NIFS Series

NIFS-156 O.J.W.F.Kardaun, J.W.P.F.Kardaun, S.-I. Itoh and K. Itoh, *Discriminant Analysis of Plasma Fusion Data*; Jun. 1992

NIFS-157 K. Itoh, S.-I. Itoh, A. Fukuyama and S. Tsuji, *Critical Issues and Experimental Examination on Sawtooth and Disruption Physics*; Jun. 1992

NIFS-158 K. Itoh and S.-I. Itoh, *Transition to H-Mode by Energetic Electrons*; July 1992

NIFS-159 K. Itoh, S.-I. Itoh and A. Fukuyama, *Steady State Tokamak Sustained by Bootstrap Current Without Seed Current*; July 1992

NIFS-160 H. Sanuki, K. Itoh and S.-I. Itoh, *Effects of Nonclassical Ion Losses on Radial Electric Field in CHS Torsatron/Heliotron*; July 1992

NIFS-161 O. Motojima, K. Akaishi, K. Fujii, S. Fujiwaka, S. Imagawa, H. Ji, H. Kaneko, S. Kitagawa, Y. Kubota, K. Matsuoka, T. Mito, S. Morimoto, A. Nishimura, K. Nishimura, N. Noda, I. Ohtake, N. Ohyabu, S. Okamura, A. Sagara, M. Sakamoto, S. Satoh, T. Satow, K. Takahata, H. Tamura, S. Tanahashi, T. Tsuzuki, S. Yamada, H. Yamada, K. Yamazaki, N. Yanagi, H. Yonezu, J. Yamamoto, M. Fujiwara and A. Iiyoshi, *Physics and Engineering Design Studies on Large Helical Device*; Aug. 1992

NIFS-162 V. D. Pustovitov, *Refined Theory of Diamagnetic Effect in Stellarators;* Aug. 1992

NIFS-163 K. Itoh, *A Review on Application of MHD Theory to Plasma Boundary Problems in Tokamaks*; Aug. 1992

NIFS-164 Y.Kondoh and T.Sato, *Thought Analysis on Self-Organization Theories of MHD Plasma*; Aug. 1992

NIFS-165 T. Seki, R. Kumazawa, T. Watari, M. Ono, Y. Yasaka, F. Shimpo, A. Ando, O. Kaneko, Y. Oka, K. Adati, R. Akiyama, Y. Hamada, S. Hidekuma, S. Hirokura, K. Ida, A. Karita, K. Kawahata, Y. Kawasumi, Y. Kitoh, T. Kohmoto, M. Kojima, K. Masai, S. Morita, K. Narihara, Y. Ogawa, K. Ohkubo, S. Okajima, T. Ozaki, M. Sakamoto, M. Sasao, K. Sato, K. N. Sato, H. Takahashi, Y. Taniguchi, K. Toi and T. Tsuzuki, *High Frequency Ion Bernstein Wave Heating Experiment on JIPP T-IIU Tokamak*; Aug. 1992

NIFS-166 Vo Hong Anh and Nguyen Tien Dung, *A Synergetic Treatment of the Vortices Behaviour of a Plasma with Viscosity*; Sep. 1992

NIFS-167 K. Watanabe and T. Sato, *A Triggering Mechanism of Fast Crash in Sawtooth Oscillation*; Sep. 1992

NIFS-168 T. Hayashi, T. Sato, W. Lotz, P. Merkel, J. Nührenberg, U. Schwenn and E. Strumberger, *3D MHD Study of Helias and Heliotron;* Sep. 1992

NIFS-169 N. Nakajima, K. Ichiguchi, K. Watanabe, H. Sugama, M. Okamoto, M. Wakatani, Y. Nakamura and C. Z. Cheng, *Neoclassical Current and Related MHD Stability, Gap Modes, and Radial Electric Field Effects in Heliotron and Torsatron Plasmas;* Sep. 1992

NIFS-170 H. Sugama, M. Okamoto and M. Wakatani, *K- ε Model of Anomalous Transport in Resistive Interchange Turbulence* ; Sep, 1992

NIFS-171 H. Sugama, M. Okamoto and M. Wakatani, *Vlasov Equation in the Stochastic Magnetic Field* ; Sep. 1992

NIFS-172 N. Nakajima, M. Okamoto and M. Fujiwara, *Physical Mechanism of E_ψ-Driven Current in Asymmetric Toroidal Systems* ; Sep.1992

NIFS-173 N. Nakajima, J. Todoroki and M. Okamoto, *On Relation between Hamada and Boozer Magnetic Coordinate System* ; Sep. 1992

NIFS-174 K. Ichiguchi, N. Nakajima, M. Okamoto, Y. Nakamura and M. Wakatani, *Effects of Net Toroidal Current on Mercier Criterion in the Large Helical Device* ; Sep. 1992

NIFS-175 S. -I. Itoh, K. Itoh and A. Fukuyama, *Modelling of ELMs and Dynamic Responses of the H-Mode* ; Sep. 1992

NIFS-176 K. Itoh, S.-I. Itoh, A. Fukuyama, H. Sanuki, K. Ichiguchi and J. Todoroki, *Improved Models of β-Limit, Anomalous Transport and Radial Electric Field with Loss Cone Loss in Heliotron / Torsatron* ; Sep. 1992

NIFS-177 N. Ohyabu, K. Yamazaki, I. Katanuma, H. Ji, T. Watanabe, K. Watanabe, H. Akao, K. Akaishi, T. Ono, H. Kaneko, T. Kawamura, Y. Kubota, N. Noda, A. Sagara, O. Motojima, M. Fujiwara and A. Iiyoshi, *Design Study of LHD Helical Divertor and High Temperature Divertor Plasma Operation* ; Sep. 1992

NIFS-178 H. Sanuki, K. Itoh and S.-I. Itoh, *Selfconsistent Analysis of Radial Electric Field and Fast Ion Losses in CHS Torsatron / Heliotron* ; Sep. 1992

NIFS-179 K. Toi, S. Morita, K. Kawahata, K. Ida, T. Watari, R. Kumazawa, A. Ando, Y. Oka, K. Ohkubo, Y. Hamada, K. Adati, R. Akiyama,

S. Hidekuma, S. Hirokura, O. Kaneko, T. Kawamoto, Y. Kawasumi, M. Kojima, T. Kuroda, K. Masai, K. Narihara, Y. Ogawa, S. Okajima, M. Sakamoto, M. Sasao, K. Sato, K. N. Sato, T. Seki, F. Shimpo, S. Tanahashi, Y. Taniguchi, T. Tsuzuki, *New Features of L-H Transition in Limiter H-Modes of JIPP T-IIU* ; Sep. 1992

NIFS-180 H. Momota, Y. Tomita, A. Ishida, Y. Kohzaki, M. Ohnishi, S. Ohi, Y. Nakao and M. Nishikawa, *D-^{3}He Fueled FRC Reactor "Artemis-L"* ; Sep. 1992

NIFS-181 T. Watari, R. Kumazawa, T. Seki, Y. Yasaka, A. Ando, Y. Oka, O. Kaneko, K. Adati, R. Akiyama, Y. Hamada, S. Hidekuma, S. Hirokura, K. Ida, K. Kawahata, T. Kawamoto, Y. Kawasumi, S. Kitagawa, M. Kojima, T. Kuroda, K. Masai, S. Morita, K. Narihara, Y. Ogawa, K. Ohkubo, S. Okajima, T. Ozaki, M. Sakamoto, M. Sasao, K. Sato, K. N. Sato, F. Shimpo, H. Takahashi, S. Tanahasi, Y. Taniguchi, K. Toi, T. Tsuzuki and M. Ono, *The New Features of Ion Bernstein Wave Heating in JIPP T-IIU Tokamak*; Sep, 1992

NIFS-182 K. Itoh, H. Sanuki and S.-I. Itoh, *Effect of Alpha Particles on Radial Electric Field Structure in Torsatron / Heliotron Reactor*; Sep. 1992

NIFS-183 S. Morimoto, M. Sato, H. Yamada, H. Ji, S. Okamura, S. Kubo, O. Motojima, M. Murakami, T. C. Jernigan, T. S. Bigelow, A. C. England, R. S. Isler, J. F. Lyon, C. H. Ma, D. A. Rasmussen, C. R. Schaich, J. B. Wilgen and J. L. Yarber, *Long Pulse Discharges Sustained by Second Harmonic Electron Cyclotron Heating Using a 35GH$_Z$ Gyrotron in the Advanced Toroidal Facility*; Sep. 1992

NIFS-184 S. Okamura, K. Hanatani, K. Nishimura, R. Akiyama, T. Amano, H. Arimoto, M. Fujiwara, M. Hosokawa, K. Ida, H. Idei, H. Iguchi, O. Kaneko, T. Kawamoto, S. Kubo, R. Kumazawa, K. Matsuoka, S. Morita, O. Motojima, T. Mutoh, N. Nakajima, N. Noda, M. Okamoto, T. Ozaki, A. Sagara, S. Sakakibara, H. Sanuki, T. Saki, T. Shoji, F. Shimbo, C. Takahashi, Y. Takeiri, Y. Takita, K. Toi, K. Tsumori, M. Ueda, T. Watari, H. Yamada and I. Yamada, *Heating Experiments Using Neutral Beams with Variable Injection Angle and ICRF Waves in CHS* ; Sep. 1992

NIFS-185 H. Yamada, S. Morita, K. Ida, S. Okamura, H. Iguchi, S. Sakakibara, K. Nishimura, R. Akiyama, H. Arimoto, M. Fujiwara, K. Hanatani, S. P. Hirshman, K. Ichiguchi, H. Idei, O. Kaneko, T. Kawamoto, S. Kubo, D. K. Lee, K. Matsuoka, O, Motojima, T. Ozaki, V. D. Pustovitov, A. Sagara, H. Sanuki, T. Shoji, C. Takahashi, Y. Takeiri, Y. Takita, S. Tanahashi, J. Todoroki, K. Toi, K. Tsumori, M. Ueda and I. Yamada, *MHD and Confinement Characteristics in the High-β Regime on the CHS Low-Aspect-Ratio Heliotron / Torsatron* ; Sep. 1992

NIFS-186 S. Morita, H. Yamada, H. Iguchi, K. Adati, R. Akiyama, H. Arimoto, M. Fujiwara, Y. Hamada, K. Ida, H. Idei, O. Kaneko, K. Kawahata, T. Kawamoto, S. Kubo, R. Kumazawa, K. Matsuoka, T. Morisaki, K. Nishimura, S. Okamura, T. Ozaki, T. Seki, M. Sakurai, S, Sakakibara, A. Sagara, C. Takahashi, Y. Takeiri, H. Takenaga, Y. Takita, K. Toi, K. Tsumori, K. Uchino, M. Ueda, T. Watari, I. Yamada, *A Role of Neutral Hydrogen in CHS Plasmas with Reheat and Collapse and Comparison with JIPP T-IIU Tokamak Plasmas* ; Sep. 1992

NIFS-187 K. Ioth, S.-I. Itoh, A. Fukuyama, M. Yagi and M. Azumi, *Model of the L-Mode Confinement in Tokamaks* ; Sep. 1992

NIFS-188 K. Itoh, A. Fukuyama and S.-I. Itoh, *Beta-Limiting Phenomena in High-Aspect-Ratio Toroidal Helical Plasmas*; Oct. 1992

NIFS-189 K. Itoh, S. -I. Itoh and A. Fukuyama, *Cross Field Ion Motion at Sawtooth Crash* ; Oct. 1992

NIFS-190 N. Noda, Y. Kubota, A. Sagara, N. Ohyabu, K. Akaishi, H. Ji, O. Motojima, M. Hashiba, I. Fujita, T. Hino, T. Yamashina, T. Matsuda, T. Sogabe, T. Matsumoto, K. Kuroda, S. Yamazaki, H. Ise, J. Adachi and T. Suzuki, *Design Study on Divertor Plates of Large Helical Device (LHD)* ; Oct. 1992

NIFS-191 Y. Kondoh, Y. Hosaka and K. Ishii, *Kernel Optimum Nearly-Analytical Discretization (KOND) Algorithm Applied to Parabolic and Hyperbolic Equations* : Oct. 1992

NIFS-192 K. Itoh, M. Yagi, S.-I. Itoh, A. Fukuyama and M. Azumi, *L-Mode Confinement Model Based on Transport-MHD Theory in Tokamaks* ; Oct. 1992

NIFS-193 T. Watari, *Review of Japanese Results on Heating and Current Drive* ; Oct. 1992

NIFS-194 Y. Kondoh, *Eigenfunction for Dissipative Dynamics Operator and Attractor of Dissipative Structure* ; Oct. 1992

NIFS-195 T. Watanabe, H. Oya, K. Watanabe and T. Sato, *Comprehensive Simulation Study on Local and Global Development of Auroral Arcs and Field-Aligned Potentials* ; Oct. 1992

NIFS-196 T. Mori, K. Akaishi, Y. Kubota, O. Motojima, M. Mushiaki, Y. Funato and Y. Hanaoka, *Pumping Experiment of Water on B and LaB_6 Films with Electron Beam Evaporator* ; Oct., 1992